Journal of Ovarian Research

RESEARCH Open Access

A novel heterozygous missense variant of *PANX1* causes human oocyte death and female infertility

Juepu Zhou[1], Ruolin Mao[1], Meng Wang[1], Rui Long[1], Limin Gao[1], Xiangfei Wang[1], Lei Jin[1*] and Lixia Zhu[1*]

Abstract
Pannexin1 (PANX1) is a highly glycosylated membrane channel-forming protein, which has been found to implicate in multiple physiological and pathophysiological functions. Variants in the *PANX1* gene have been reported to be associated with oocyte death and recurrent in vitro fertilization failure. In this study, we identified a novel heterozygous *PANX1* variant (NM_015368.4 c.410 C>T (p.Ser137Leu)) associated with the phenotype of oocyte death in a non-consanguineous family, followed by an autosomal dominant (AD) mode. We explored the molecular mechanism of the novel variant and the variant c.976_978del (p.Asn326del) that we reported previously. Both of the variants altered the PANX1 glycosylation pattern in cultured cells, led to aberrant PANX1 channel activation, affected ATP release and membrane electrophysiological properties, which resulted in mouse and human oocyte death in vitro. For the first time, we presented the direct evidence of the effect of the *PANX1* variants on human oocyte development. Our findings expand the variant spectrum of *PANX1* genes associated with oocyte death and provide new support for the genetic diagnosis of female infertility.

Keywords *PANX1*, Variant, Oocyte death, Female infertility

Introduction

Successful mammalian reproduction requires normal spermatogenesis, oogenesis, fertilization, and early embryonic development, and defects in any of these processes will result in infertility, recurrent miscarriage, or even birth defects [1–4]. In recent years, infertility has been recognized as a long-standing problem and has become more common in the world [5]. Since the first in vitro fertilization (IVF) procedure performed in 1978, assisted reproductive technology (ART) has become a routine treatment for infertility individuals, and it is now estimated that more than six million babies have been delivered by IVF and intracytoplasmic sperm injection (ICSI) [6]. However, there are still many factors leading to recurrent failure of IVF/ICSI attempts. With the development of ART and advanced genetic assays, it was found that many infertile female patients were caused by variants in various developmental regulators, such as *PATL2* [7, 8], *TUBB8* [9, 10], *PADI6* [11], et al. These genetic factors have been identified as potential markers for evaluating oocyte quality and providing individualized genetic counseling [6].

Pannexin1 (PANX1), which belongs to integral membrane proteins family pannexins, is a highly glycosylated membrane protein [12]. It exists as three species: the non-glycosylated protein (GLY0), the high mannose-type

*Correspondence:
Lei Jin
leijintongjih@qq.com
Lixia Zhu
zhulixia027@163.com
[1]Reproductive Medicine Center, Tongji Hospital, Tongji Medical College, Huazhong University of Science and Technology, No.1095, Jiefang Road, Wuhan 430030, China

glycoprotein (GLY1), and the fully processed glycoprotein (GLY2) [13]. As a major ATP release and nucleotide permeation channel, PANX1 has been found to implicate in multiple physiological and pathophysiological functions, such as inflammatory response [14], cancer progression and metastasis [15], ischemia [16], neurological disorders [17], et al. Recent studies have also found that PANX1 is associated with female infertility [18]. Variants in *PANX1* led to cytoplasmic shrinkage, darkening and death of oocytes before or after fertilization, which was defined as "oocyte death" phenotype [18–20]. Preliminary research indicated that variants altered the PANX1 glycosylation pattern, thus resulting in aberrant PANX1 channel activity and ATP release, which negatively affect the development of oocytes [18]. Despite that, the mechanism research on *PANX1* variants and oocyte death is far from completeness and needs continuous exploration.

In our previous work, we preliminary reported a novel *PANX1* variant c.976_978del (p.Asn326del) [21]. Recently, we identified another novel *PANX1* variant c.410 C>T (p.Ser137Leu). In this study, we comprehensively investigated the effects of these two variants of *PANX1* in cultured cells, in mouse oocytes, and in human oocytes. This study explores the mechanism of oocyte death related to *PANX1* variants, and expands the variant spectrum of *PANX1*.

Materials and methods

Human subjects and ethics approval

Infertility patients diagnosed with the oocyte death phenotype were recruited from the Center of Reproductive Medicine, Tongji Hospital, Tongji Medical College, Huazhong University of Science and Technology. Participants with normal oocytes and embryos in IVF/ICSI cycles were also recruited as the control group. All oocytes and embryos from controls and patients were obtained with written informed consent signed by the donor couples.

This study was approved by the ethics committee on human subject research at Tongji Hospital, Huazhong University of Science and Technology (TJ-IRB20220450). The animal experiments were approved by the Animal Welfare and Ethics Committee of Tongji Hospital (TJH-202,210,011).

Wholeexome sequencing (WES) and Sanger sequencing

Genomic DNA was extracted from peripheral blood samples of the patients and their members for WES to identify potential disease-causing variants according to the manufacturer's instructions. The details of the genetic analysis procedure have been well described previously [10, 22]. Candidate variants identified in the participants were validated by Sanger sequencing analyses conducted on ABI PRISM 3500 Genetic Analyzer (Applied Biosystems, Foster City, CA).

The specific filtering process of variant sites was as follows: (a) The variant sites in the 1000 Genomes database and Exome Aggregation Consortium (frequency>0.01 in the population) were filtered, and the inter-individual diversity sites were removed to obtain rare variants that may actually cause disease; (b) The variant sites of exonic region or splicing site region (10 bp upstream/downstream) were retained; (c) Synonymous variants (without changing amino acids) were removed to obtain variants that affect gene expression products; (d) The variant sites predicted to have an impact on protein structure or function in more than 2 online variants prediction tools were retained; (e) Screen variations in genes associated with female infertility. At last, we could lock the variants consistent with clinical phenotype and genetic pattern. The details on variant selection were showed in the supplementary table.

Variants analysis and molecular modelling

Evolutionary conservation was assessed using Clustal Omega software (https://www.ebi.ac.uk/Tools/msa/clustalo/). The allele frequency of the variants in the general population was assessed using Genome Aggregation Database (GnomAD, http://gnomad.broadinstitute.org/). The pathogenicity of the variant was assessed using three online software: sorting intolerant from tolerant (SIFT, sift.jcvi.org), polymorphism phenotyping (PloyPhen2, genetics.bwh.harvard.edu/pph2), and mutation taster (http://www.mutaiontaster.org/). The structure model was built based on Cryo-EM structure of wild-type human pannexin1 channel (PDB ID, 6WBF/A) in the RCSB Protein Data Bank (https://www.rcsb.org/). PyMOL software (https://pymol.org/2/) was used to analyze the effect of the variants in PANX1 protein.

Expression vector construction

Wild-type (WT) human *PANX1* and mutated *PANX1* (p.Asn326del, p.Ser137Leu) were constructed and then recombined with the eukaryotic expression vector pcDNA3.1. A 3×FLAGtag was fused at the C-terminus of WT and mutated *PANX1*, respectively. The plasmids were constructed by OBiO Technology (Shanghai).

Cell culture and transfection

HeLa cells were obtained from Cancer Biology Research Center of Tongji Hospital, Tongji Medical College, Huazhong University of Science and Technology. Cells were cultured in Dulbecco's Modifed Eagle Medium/Nutrient Mixture F-12 (DMEM/F-12, KeyGEN Bio TECH, Jiangsu, China) supplemented with 1% penicillin/ streptomycin (Servicebio, Wuhan, China) and 10% (v/v) fetal bovine serum (FBS, Wisten, Nanjing, China)

in a humidified incubator with a 5% CO_2 atmosphere at 37 °C. *PANX1* WT and mutant constructs were transfected into HeLa cells using liposomal transfection reagent (Yeasen, Shanghai, China) according to the manufacturer's instructions.

Western blotting

HeLa cells were harvested 36 h after transfection and washed three times with cold phosphate-buffered saline (PBS, Servicebio, Wuhan, China). Cells were lysed in RIPA lysis buffer with 2% of protease inhibitor (Servicebio, Wuhan, China). After incubating on the ice for 20 min and centrifuging at 12,000 rpm at 4 °C for 20 min, protein lysates were collected in a new centrifuge tube. Protein concentrations were determined with a BCA protein quantitative detection kit (Servicebio, Wuhan, China). Then, cell extracts were mixed with 5×sodium dodecyl sulfate (SDS) loading buffer (Servicebio, Wuhan, China) and denatured by boiling at 100 ℃ for 10 min. Equal amounts of protein were separated by 10% sodium dodecyl sulfate-polyacrylamide gel electrophoresis (SDS-PAGE) and transferred to nitrocellulose filter membranes (Merck KGaA, Darmstadt, Germany). The membranes were blocked in 5% skim milk diluted in 1× Tris-buffered saline (Servicebio, Wuhan, China) with 0.1% Tween 20 (TBST, Servicebio, Wuhan, China) for 1 h and incubated at 4 °C overnight with rabbit anti-PANX1 (1:1000 dilution, Cell Signaling Technology, kind gifts from Lei Wang's lab in Fudan University) or rabbit anti-vinculin (1:1000 dilution, ABclonal, Wuhan, China) antibodies. After incubation with the goat anti-rabbit IgG secondary antibodies (1:2000 dilution, Servicebio, Wuhan, China) for 1 h at room temperature on the secondary day, the membranes were detected by ECL chemiluminescence kit (Vazyme, Nanjing, China) and imaged on a chemiluminescent imaging system (GeneGnome XRQ, Syngene, England). For densitometric analyses, protein bands on the blots were measured by ImageJ software.

Complementary RNAs (cRNAs) transcription

WT and mutant *PANX1* cRNAs (RNA transcripted from complementary DNA) was constructed by GenScript (Nanjing, China). Briefly, WT and mutant constructs were linearized by digestion with the AgeI restriction enzyme, then purified linearized DNA was used as a template to transcribe *PANX1* cRNAs.

Collection and microinjection of mouse GV oocytes and fertilized oocytes

For GV oocytes collection, ovaries were isolated from 6 to 8-week-old Kun-Ming (KM) female mice (Biont, Hubei, China). Germinal vesicle (GV) oocytes were harvested by puncturing the large ovarian follicles and collected by mouth pipetting on the stage of a dissecting microscope. The GV oocytes were cultured in M2 medium (Aibei Biotechnology, Nanjing, China) under mineral oil (Servicebio, Wuhan, China) in an atmosphere of 5% CO_2 at 37 °C.

For fertilized oocytes collection, the 6 to 8-week-old KM female mice were injected with 7.5 IU pregnant mare serum gonadotropin (PMSG, Aibei Biotechnology, Nanjing, China). 44–48 h after PMSG injection, each mouse was injected with 7.5 IU human chorionic gonadotropin (hCG, Aibei Biotechnology, Nanjing, China), and the mice were then euthanized after 14 h. Oviducts were removed and transferred to a pre-warmed human tubal fluid (HTF, Aibei Biotechnology, Nanjing, China) medium. Then cumulus oophorus masses (COMs) containing oocytes were removed by dissecting oviducts and transferred to the HTF medium. For sperm collection, 10 to 12-week-old male mice were euthanized, and the epididymal tails were taken out and transferred to a pre-warmed HTF medium. Scratches were made on the tails of the epididymis by an insulin needle to allow sperms to escape. Then they were incubated for 1 h to complete the capacitation. Finally, COMs were mixed with sperms in HTF for fertilization. Two pronuclei (2PN) zygotes were collected 6 h after fertilization.

The collected mouse GV oocytes and fertilized oocytes were microinjected with WT or mutant *PANX1* cRNAs using a Narishige micromanipulator. About 5 to 10 pl of cRNA solution (250 to 1000 ng/μl) was microinjected into the cytoplasm of each mouse oocyte. Injected GV oocytes were matured in vitro in M2 medium (Sigma-Aldrich, USA) for 12 h, and the morphological changes of oocytes were recorded. Injected zygotes were cultured in KSOM medium (Aibei Biotechnology, Nanjing, China) for 12 h, and the morphological changes and embryo development were recorded. All oocytes and zygotes were cultured at 37 °C in an atmosphere of 5% CO_2. For PANX1 channel inhibition experiments, carbenoxolone (CBX, MedChemExpress, Shanghai, China) was used at a concentration of 300 μM.

Mouse oocyte ATP measurements

Mouse GV oocytes were cultured in 80 μl of M2 medium containing 300 μM ARL 67,156 trisodium (Sigma-Aldrich, USA) with or without 300 μM CBX, and collected at 6 h after injection with WT or mutant *PANX1* cRNAs. The relative ATP content was determined with the Enhanced ATP Assay Kit (Beyotime, Shanghai, China). For extracellular ATP measurements, a mixture of 50 μl of culture medium and 50 μl of ATP assay reagent was assayed using a luminometer (Servicebio, Wuhan, China). For intracellular ATP measurement, 20 GV oocytes were lysed with 100 μl of ATP assay lysis buffer for 10 min and centrifuged at 4000 g at room temperature for 30 s. A mixture of 50 μl of supernatant and 50 μl of ATP assay reagent was assayed using the luminometer.

The relative ATP concentration was expressed as a ratio of all values with respect to the WT group.

Mouse oocyte cell membrane potentials measurements

Mouse GV oocytes were cultured in M2 medium with or without 300 μM CBX, and collected at 6 h after injection with WT or mutant *PANX1* cRNAs. Oocytes were first incubated with Hoechst33342 (Servicebio, Wuhan, China) for 5 min and washed three times with M2 medium. Oocytes were then incubated with M2 medium containing 5 μM cell membrane potential sensitive fluorescent dye DiBAC4 [3] (MedChemExpress, Shanghai, China) and immediately examined and photographed under confocal laser scanning microscope (Zeiss LSM 510 META, Germany). The relative fluorescence intensity was measured by ImageJ and expressed as a ratio of all values with respect to the WT group.

Microinjection of human oocytes

Human GV oocytes were collected from ICSI patients on the day of oocyte retrieval after denudation. And 3PN fertilized oocytes were collected from IVF patients one day later after fertilization ascertainment. All patients in our center donating oocytes for research were informed and signed written consent. The microinjection procedure was similar to that of mice. Briefly, about 8 to 10 pl of cRNA solution (1000 ng/μl) was microinjected into the cytoplasm of each human GV oocyte and pronucleus oocyte. Then the injected oocytes were cultured in a time-lapse incubator with 6% CO_2 and 5% O_2 at 37 ℃. The morphological changes of oocytes and subsequent embryonic development were recorded accordingly.

Immunofluorescence staining

The oocytes and embryos were collected and fixed with 4% (w/v) paraformaldehyde in PBS for 1 h at room temperature, and then were permeabilized in PBS containing 0.1% (w/v) Triton X-100 and 1% BSA for 30 min at room temperature. After washing three times with PBS containing 1% BSA, oocytes and embryos were incubated in blocking solution (PBS containing 3% BSA) for 1 h at room temperature. Then oocytes and embryos were incubated at 4 ℃ overnight with rabbit anti-PANX1 (1:100 dilution, Sigma-Aldrich, kind gifts from Lei Wang's lab in Fudan University) antibody. On the second day, oocytes and embryos were incubated with FITC-labeled secondary antibody (1:100 dilution, Servicebio, Wuhan, China) for 1 h. After washing three times, oocytes and embryos were incubated with Tubulin-Tracker Red (Beyotime, Shanghai, China) for 30 min at room temperature. Then oocytes and embryos were incubated with 4′,6-diamidino-2-phenylindole (DAPI, Servicebio, Wuhan, China) for 20 min at room temperature. Finally, the samples were mounted on glass slides and examined with a confocal laser scanning microscope (Zeiss LSM 510 META, Germany).

Statistics

All data are representative of three independent experiments. GraphPad Prism (version 9.0) was used to perform the statistical analysis. Values were analyzed by Student's t-tests when comparing experimental groups. Wald p-values were two-sided; $p<0.05$ was considered to be statistically significant.

Results

Clinical characteristics of the probands

Two probands from two independent families have been diagnosed with primary infertility for several years (Fig. 1). The basic information and clinical history of the proband (II-1) in family 1 were reported in detail in our previous publication [21]. The proband (II-1) in family 2 was a 30-year-old woman with 6-year history of unexplained primary infertility at examination. She had normal ovarian reserves and normal levels of sex hormones with basal follicle-stimulating hormone (FSH) 7.53 mIU/mL, luteinizing hormone (LH) 5.7 mIU/mL, and anti-Mullerian hormone (AMH) 3.89 ng/mL. The seminal parameters of her husband showed 51.3 million per milliliter of sperm concentration, 56.1% progressive motility, and 4.6% normal sperm morphology per ejaculate. The chromosome karyotypes of the couple were normal. She had undergone one failed IVF Table 1, . In this IVF cycle, she underwent a gonadotropin-releasing hormone agonist (GnRH-a) protocol. The estradiol level on the day of hCG trigger was 1320.0 pg/ml. A total of 15 oocytes were retrieved, 8 of the 12 MII stage oocytes were successfully fertilized. However, all the fertilized oocytes became shrinking in the subsequent culture, degenerated and died within 40 h (Fig. 2A).

Identification of variants in *PANX1*

It has been reported that pathogenic variants in *PANX1* can cause female infertility characterized by the oocyte death phenotype [18]. Because of the oocyte death phenotype observed in the probands of the two families, screening of *PANX1* variants was performed. After WES and Sanger sequencing, we found two novel variants of *PANX1*, and no variants were identified in any other known disease-causing genes related to female infertility or other genes related to oocyte development. The proband in family 1 had a heterozygous deletion variant c.976_978del (p.Asn326del), which was inherited from her father, as previously described [21]. The proband in family 2 had a heterozygous missense variant c.410 C>T (p.Ser137Leu). This is a suspected de novo variant because her parents did not carry the variant of *PANX1* (Fig. 1A and B). However, due to sample limitations,

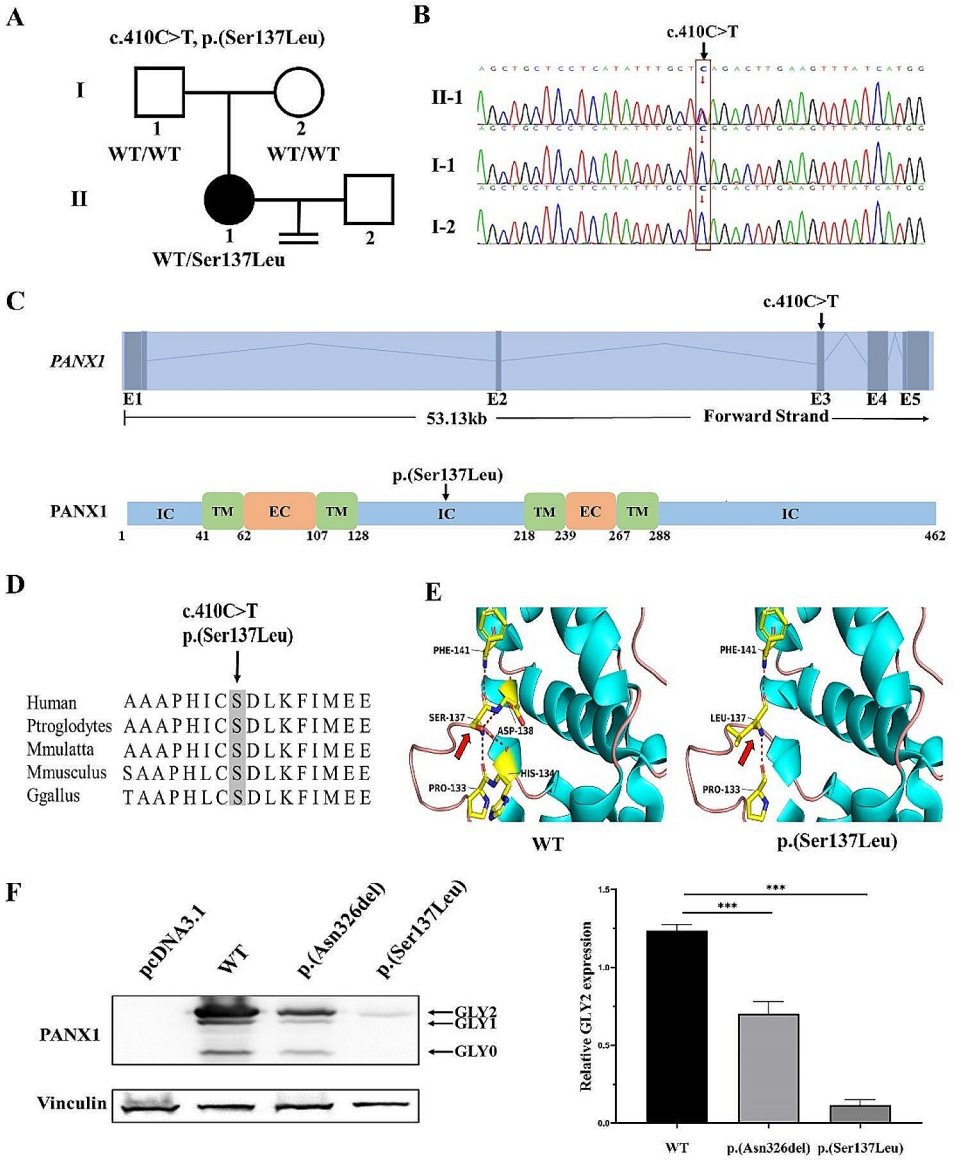

Fig. 1 Identification of variant in *PANX1*. **A** A pedigree carrying *PANX1* variant that lead to infertility. Squares indicate male family member, circles indicate female members, black solid circle indicates the proband, the equal sign indicates infertility, and "WT" indicates wild-type allele. **B** Sanger sequencing results of the proband and her family members. **C** Location of the newly identified heterozygous variant in *PANX1* exon and PANX1 protein. TM, transmembrane region; EC, extracellular region; IC, intracellular region. **D** Conservation analysis of the affected amino acid among different species. **E** PyMOL-predicted structures of *PANX1* variant. The structures of wild-type and mutated PANX1 proteins were modeled based on Cryo-EM structure of wild type human pannexin1 channel (PDB ID, 6WBF/A). Red arrows indicate the variant; "WT" indicates wild-type allele. **F** Western blot analysis of HeLa cell extracts after transfection with WT or mutant PANX1 constructs. Vinculin was used as the loading control. The relative GLY2 expression of two variants was significantly reduced compared with WT. Three independent experiments were performed; ***$P < 0.001$. WT, wild type

paternity and maternity testing cannot be performed, so it is not clear whether this variant is a de novo variant.

Function prediction of the *PANX1* variant

Function prediction of variant c.976_978del were reported in detail in our previous publication [21]. Variant c.410 C>T is located in exon 3 and caused alteration of serine to leucine at position 137 of PANX1 protein. The residue Ser137 was highly conserved across species (Fig. 1C and D). As shown in Table 2, the variant c.410 C>T is absent in the GnomAD. It was predicted to be damaging by SIFT, probably damaging by PloyPhen2, and disease causing by mutation taster. We used the structure model 6WBF/A in the RCSB Protein Data Bank and PyMOL software to analyze the effect of the variant in PANX1. As shown in Fig. 1E, Ser137 can form hydrogen bonds with Pro133, His134, Asp138, and Phe 141.

Table 1 Clinical characteristics of IVF attempts of the probands

Case	Insemination method	Stimulation protocol	Total oocytes	MII oocytes	Fertilized oocytes	Oocytes that died or degenerated after fertilization	Outcomes
Family1 II-1 [21]	First IVF	Long GnRH-a	27	27	27	26	One frozen-thawed embryo was transferred but failed to implant
	Second IVF	Mild stimulation	19	18	15	14	One frozen-thawed embryo (8-cell) was transferred but failed to implant
Family2 II-1	First IVF	Long GnRH-a	15	12	8	8	Cancel transfer

GnRH-a, gonadotropin-releasing hormone (GnRH) agonist; IVF, in vitro fertilization

While Leu137 can't form hydrogen bonds with His134 and Asp138.

Effect of heterozygous variant on PANX1 glycosylation in vitro

PANX1 is a highly glycosylated membrane protein. To evaluate the effect of the heterozygous variant on PANX1 glycosylation in vitro, WT and mutated *PANX1* constructs were transfected into HeLa cells. Compared with WT *PANX1*, these two variants both resulted in a significant reduction of GLY2 expression (Fig. 1F). In addition, in our immunofluorescence experiments, PANX1 was mainly localized on the cell membrane of human control oocytes. While oocytes and embryos from the proband (Family 2, p.Ser137Leu) showed a decrease in cell membrane localization and obvious cytoplasmic aggregation (Fig. 2B). These results indicated that these two variants resulted in an altered glycosylation pattern and localization of PANX1 protein.

Mimicking the oocyte death phenotype in mouse oocytes

To mimic the phenotype of oocyte death related to *PANX1* mutations, WT and mutant *PANX1* cRNAs were microinjected into mouse GV oocytes at four different concentrations (250, 500, 700, and 1000 ng/μl). GV oocytes were then cultured in vitro for 12 h. As shown in Fig. 3A, mouse oocytes injected with mutant p.Asn326del or p.Ser137Leu cRNA gradually degenerated, with cytoplasmic shrinkage and death at 12 h. What's more, the phenotype showed a dosage-dependent effect, with a greater concentration associated with higher oocyte death rate.

Channel activation, aberrant ATP release, and altered membrane properties caused by *PANX1* variants

To determine whether the *PANX1* variants we identified cause the oocyte death phenotype by altering channel activity, we used a channel inhibitor CBX in a rescue experiment. Mutant p.Asn326del or p.Ser137Leu cRNAs were injected into mouse GV oocytes or into normal 2PN zygotes, which were then cultured in the presence or absence of CBX. In the groups free of CBX, most of the oocytes or zygotes degenerated or died within 12 h, whereas oocytes or zygotes incubated with CBX were all viable at 12 h (Fig. 3B and C). These results suggested that these two *PANX1* variants result in enhanced channel activation.

Previous studies have shown that PANX1-mediated ATP release is the main activity of PANX1 [23]. To explore whether *PANX1* variants affected ATP release, we measured the intracellular and extracellular ATP content in oocytes injected with WT or mutant cRNAs. As shown in Fig. 3D, the intracellular ATP content was significantly decreased, and the extracellular ATP content was significantly increased in groups injected with mutant cRNAs. These changes were reversed by adding CBX, confirming that channel activation is caused by the variants.

To further explore the effect of *PANX1* variants on membrane properties, we used DiBAC4 [3] to explore the changes in membrane potential. DiBAC4 [3] is a cell membrane potential sensitive lipophilic anionic fluorescent dye. Due to its negative ion characteristics, it will enter and exit the cell membrane with the change of cell membrane potential to maintain the dynamic balance of charge inside and outside the membrane. As shown in Fig. 3E, oocytes injected with mutant cRNAs exhibited a significantly enhanced fluorescence intensity, suggesting a clear elevation of cell membrane potential. This change can be reversed by CBX, indicating that the variants leads to altered membrane properties.

Mimicking the oocyte death phenotype in human oocytes and embryos

To better explore the relationship between *PANX1* variants and human oocyte death phenotype, we directly microinjected WT and mutant *PANX1* cRNAs into abandoned human GV oocytes or abnormally fertilized zygotes. Timelapse system was used to record the morphological changes of oocytes and embryos. As shown in Fig. 4, most human oocytes injected with WT or mutant cRNAs gradually degenerated with cytoplasmic shrinkage at 10 h, and death when cultured for up to 20 h. Similar to the immunofluorescence results of the proband's oocytes, the oocytes injected with mutant cRNAs showed decrease in cell membrane localization and

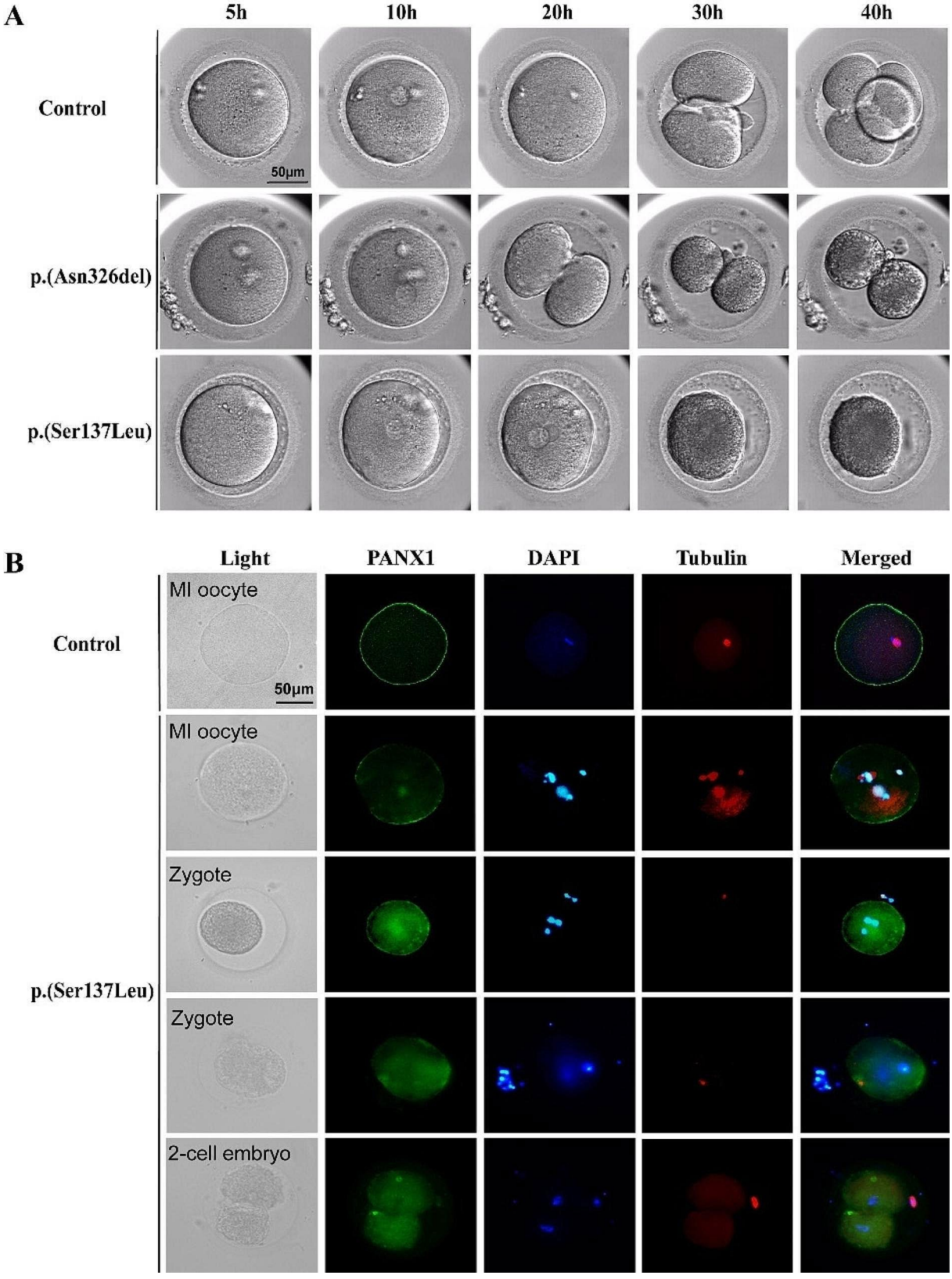

Fig. 2 Morphology and immunofluorescence of oocytes and embryos from probands. **A** Morphological change of oocytes and embryos retrieved from control individuals and probands through timelapse system. Scale bar, 50 μm. **B** Immunofluorescence staining of oocytes and embryos retrieved from control individual and the proband with p.Ser137Leu variant. Scale bar, 50 μm

Table 2 Overview of the *PANX1* variants

Genomic position on Chr11	cDNA change	Protein change	Variant type	GnomAD	SIFT	PloyPhen2	Mutation taster
93,913,198_93,913,200 [21]	c.976_978del	p.Asn326del	Deletion	Absent	NA	NA	Disease causing
93.911.623	c.410 C>T	p.Ser137Leu	Missense	Absent	Damaging	probably damaging	Disease causing

NA, not applicable

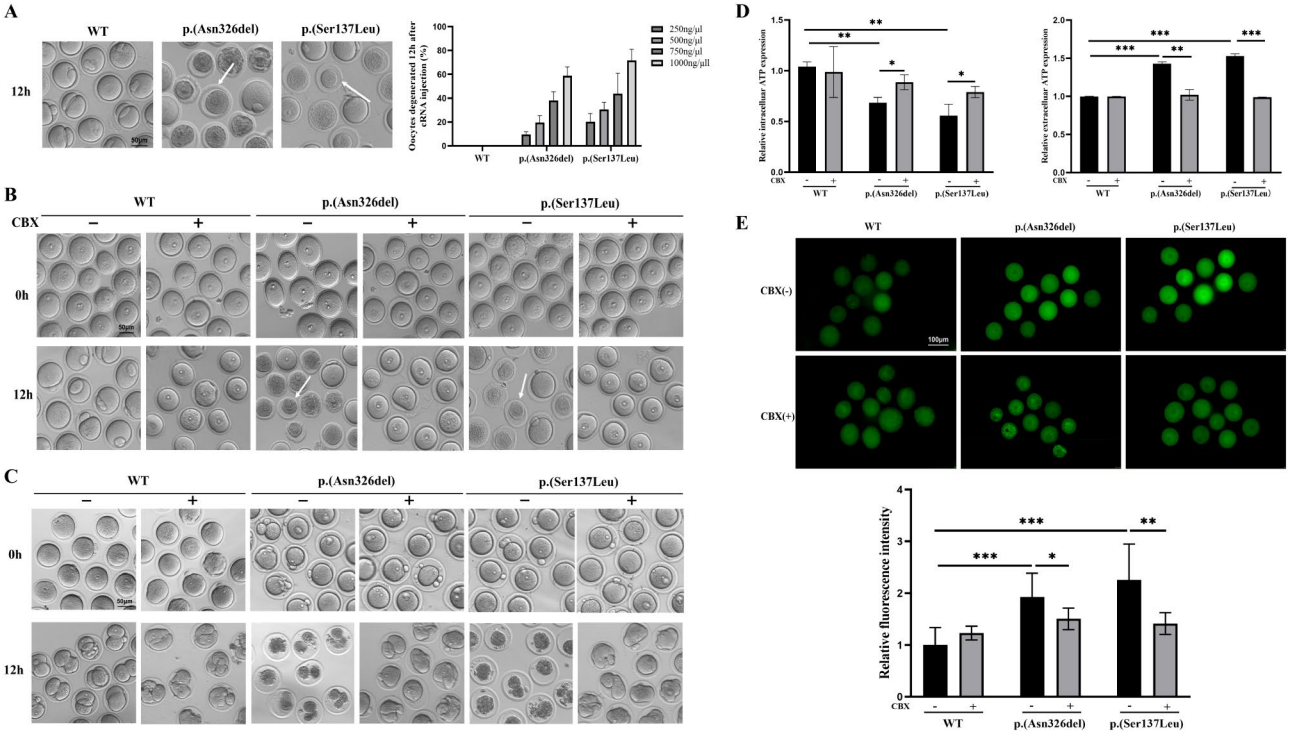

Fig. 3 Mimicking the oocyte death phenotype in mouse oocytes in vitro. **A** Images of mouse GV oocytes injected with WT or mutant cRNAs at 12 h and statistical analysis. White arrows indicate dead oocytes. Data are shown as the means ± SEM; $n = 3$ biological replicates. Scale bar, 50 μm. **B** GV oocytes were injected with WT, p.Asn326del, or p.Ser137Leu cRNAs and cultured in M2 medium either with (+) or without (–) CBX for 12 h ($n = 3$ biological replicates). White arrows indicate dead oocytes. Scale bar, 50 μm. **C** 2PN zygotes were injected with WT, p.Asn326del, or p.Ser137Leu cRNAs and cultured in KSOM medium either with (+) or without (–) CBX for 12 h ($n = 3$ biological replicates). Scale bar, 50 μm. **D** Measurement of intracellular and extracellular ATP content in oocytes injected with WT, p.Asn326del, or p.Ser137Leu cRNAs for 6 h. Data are shown as the means ± SEM; $n = 3$ biological replicates. $^{*}P < 0.05$, $^{**}P < 0.01$, $^{***}P < 0.001$. **E** Measurement of cell membrane potentials in oocytes injected with WT, p.Asn326del, or p.Ser137Leu cRNAs for 6 h. Data are shown as the means ± SEM; $n = 3$ biological replicates. $^{*}P < 0.05$, $^{**}P < 0.01$, $^{***}P < 0.001$. Scale bar, 100 μm

cytoplasmic aggregation of PANX1. This is basically the same as the phenotype of the proband. Microinjection of human zygotes also showed similar results (Fig. 5). The obvious oocyte death phenotype appeared on the first day after the microinjection of mutant cRNA, and the number of dead embryos increased on the second day, accompanied by an arrested or retarded embryo development. PANX1 was mainly localized at cell-cell interfaces of embryos in WT group. While in embryos injected with mutant cRNAs, PANX1 showed more obvious cytoplasmic localization.

Discussion

In this study, we identified a heterozygous variant c.410 C>T (p.Ser137Leu) in *PANX1* from a non-consanguineous family. Similar to the variant c.976_978del (p.Asn326del) we previously identified, oocytes showed the oocyte death phenotype after fertilization. These two variants altered the PANX1 glycosylation pattern, affected ATP release and membrane electrophysiological properties, and resulted in mouse and human oocyte death in vitro.

In recent years, with the discovery of the heptamer structure of PANX1 by cryo-electron microscopy, this membrane channel protein closely related to ATP release has received more attention [24–26]. However, although PANX1 has been found to be involved in many pathophysiological processes [27–29], its role in the reproductive field still lacks clear research. In 2019, Wang et al. first reported the identification of heterozygous *PANX1* variants in female infertility patients, and defined this new infertility phenotype as "oocyte death" [18]. Subsequently, Sang et al. reported two homozygous variants of *PANX1* caused oocyte death with an autosomal recessive

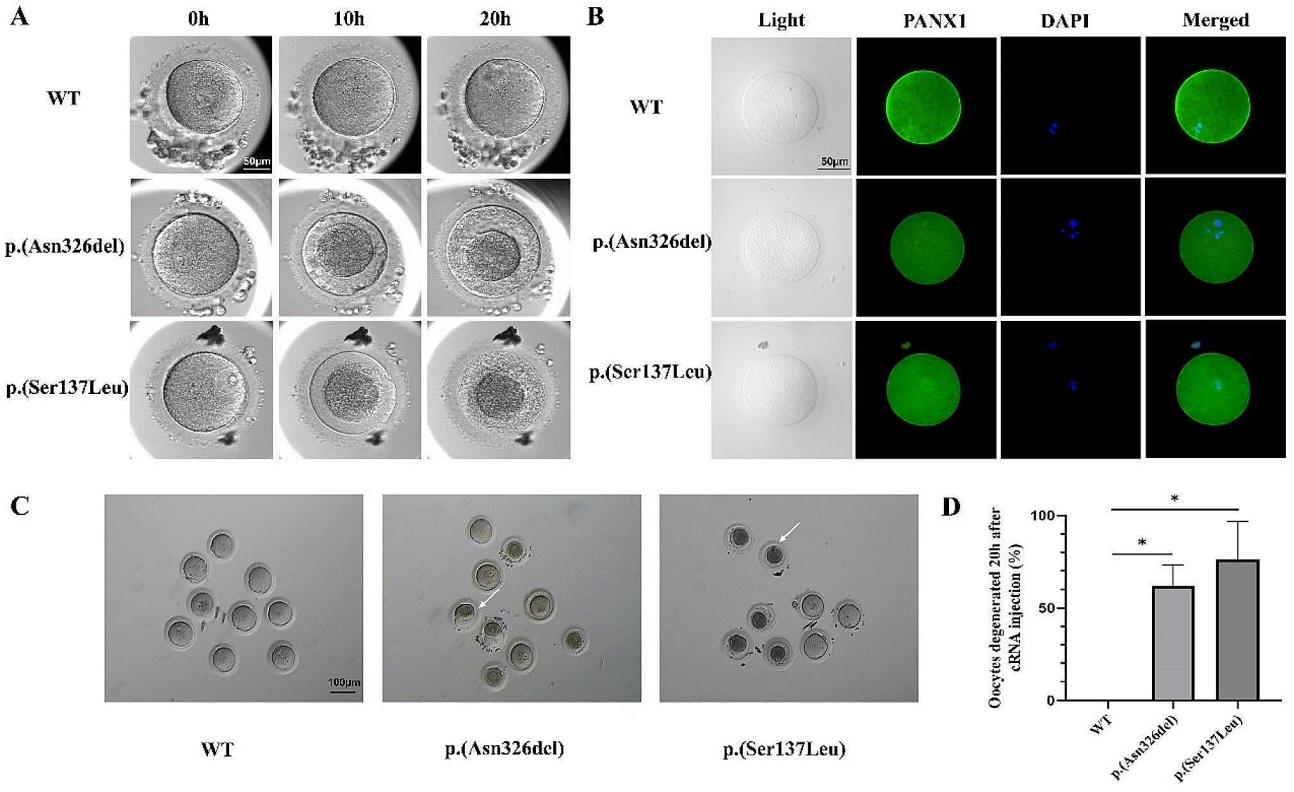

Fig. 4 Mimicking the oocyte death phenotype in human oocytes in vitro. **A** Morphological change of human GV oocytes injected with WT, p.Asn326del, or p.Ser137Leu cRNAs through timelapse system. Scale bar, 50 μm. **B** Immunofluorescence staining of oocytes injected with WT, p.Asn326del, or p.Ser137Leu cRNAs. Scale bar, 50 μm. **C** Image of oocyte death phenotype in human GV oocytes injected with WT, p.Asn326del, or p.Ser137Leu cRNAs for 20 h. Scale bar, 100 μm. **D** Statistical analysis of oocytes degenerated 20 h after cRNAs injection. $^{*}P < 0.05$

(AR) mode, and the destructive effect of the two homozygous variants on PANX1 function was weaker than that caused by the previous reported heterozygous variants [19]. Recently, Tan et al. reported the seventh identified variant of *PANX1* related to oocyte death, followed by an autosomal dominant (AD) mode with reduced penetrance [20]. In our recently identified *PANX1* variant c.976_978del (p.Asn326del), most of the oocytes died after fertilization, but there was also high-quality embryo that could be transferred [21]. The differential effects of variants sites on protein function have been analyzed in detail in our previous report on variant c.976_978del [21]. Therefore, these results indicate that different locations of variants might appear to different effects on the function of PANX1 and inheritance patterns might also be affected.

In the present study, we identified a novel *PANX1* variant c.410 C>T (p.Ser137Leu). Molecular mechanism studies suggest that variant p.Ser137Leu affects the structural stability of *PANX1*, which may lead to functional abnormalities. As the level of glycosylation is critical for the cellular localization and the function of the PANX1 channel [30], glycosylation assay is an important part of assessing PANX1 function. Similar to the previously identified variants, the variant p.Ser137Leu changed the glycosylation pattern of PANX1, thus affecting the intracellular localization of PAXN1. It is worth noting that variant p. Ser137Leu resulted in the complete deletion of GLY0 and GLY1 species, which may be due to the decrease of protein stability and early degradation caused by variant. The difference of variant sites will be further studied in the future.

Previous studies have shown that *Panx1* knockout mice have no obvious fertility defects [31]. And the engineered OE-PANX1$^{Q392^{*}}$ female mice were completely infertile with the oocyte death phenotype, implying that the oocyte death phenotype was caused by a gain-of-function effect [18]. Therefore, even in the presence of WT allele, the molecular mechanism of oocyte death caused by *PANX1* variant can still be explored by direct injection of mutant cRNAs in mouse oocyte and embryo. Oocytes and embryos injected with variant cRNAs showed oocyte death phenotype in a dose-dependent manner. Although the embryonic phenotype is similar, unlike mouse oocytes, the probands' oocytes can survive before fertilization. This phenotypic difference may be affected by species and the concentration of cRNAs injected. The use of channel inhibitor CBX can reverse

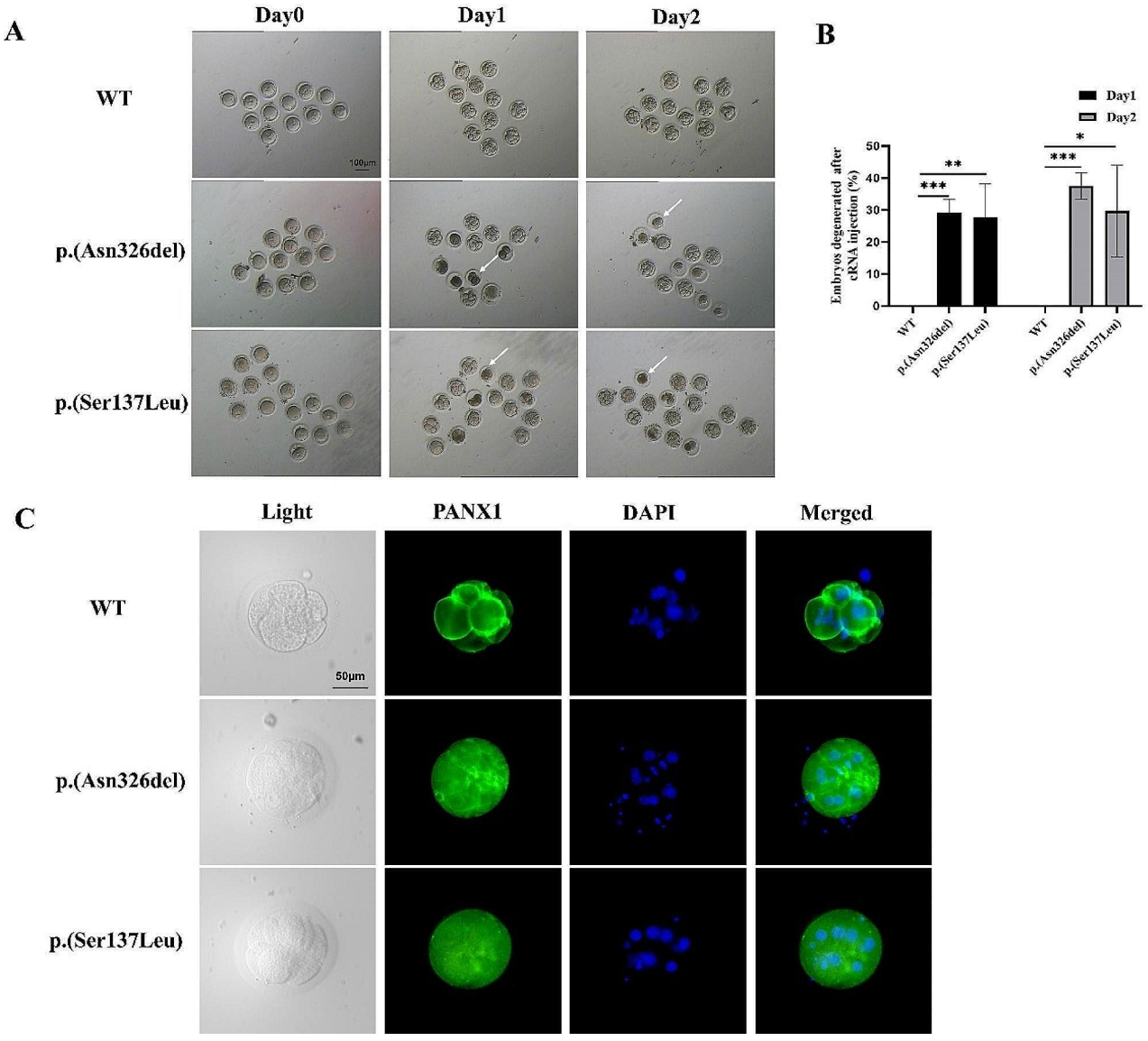

Fig. 5 Mimicking the oocyte death phenotype in human zygotes in vitro. **A** Images of embryo development of human 3PN zygotes injected with WT, p.Asn326del, or p.Ser137Leu cRNAs. Scale bar, 100 μm. **B** Statistical analysis of degenerated oocytes/embryos 1 day or 2 days after cRNAs injection. $^{*}P < 0.05$, $^{**}P < 0.01$, $^{***}P < 0.001$. **C** Immunofluorescence staining of embryos developed from 3PN zygotes injected with WT, p.Asn326del, or p.Ser137Leu cRNAs. Scale bar, 50 μm. AD, autosomal dominant; AR, autosomal recessive; VUS, variant of uncertain significance

this phenotype, suggesting that the altered channel activity of mutant PANX1 is an crucial cause of oocyte death. This altered channel activity is also reflected in the significantly enhanced cell membrane potential and disordered ATP release. Therefore, the changes of channel activity caused by variants affect the regulation of ATP release by PANX1, which ultimately leads to oocyte death.

For the first time, we further presented the direct evidence of the effect of the *PANX1* variants on human oocytes development by injecting cRNAs into human oocytes, which is of great significance for exploring the effect of species differences on oocyte death phenotype. Our study utilized human oocytes and embryos as research objects, which would be more accurate and intuitive for the observation and outcome assessment of genetic mutations. Our results further confirm that the identified heterozygous variants c.976_978del (p.Asn326del) and c.410 C>T (p.Ser137Leu) in *PANX1* are responsible for oocyte death and female infertility.

On the basis of clarifying the pathogenic genes, finding a resolved method to achieve a successful pregnancy is a more clinical concern. Successful pregnancy has been reported in some studies on infertility-related genes [32, 33]. However, despite attempts to transfer good quality embryos, the currently identified infertile patients carrying the *PANX1* variants have not yet achieved a

successful pregnancy. Our results suggest that CBX has a strong ameliorating effect on the phenotypic changes in oocytes caused by *PANX1* variants, which gives us inspiring clues in exploration the appropriate solution methods for these specific patients in the future. However, in consideration of the influence of long term inhibition of ion channels by CBX on embryo viability, the mechanism of PANX1 needs to be further studied to explore more precise therapy strategy in improving the prognosis of such patients.

Conclusion

In conclusion, we have identified the heterozygous variant c.410 C>T (p.Ser137Leu) in *PANX1* as responsible for oocyte death and female infertility. Our finding expands the variant spectrum of *PANX1* and provides additional genetic markers for infertility patients.

Supplementary Information

The online version contains supplementary material available at https://doi.org/10.1186/s13048-024-01462-9.

Supplementary Material 1

Acknowledgements
We would like to thank Dr. Qing Sang and Dr. Lei Wang from Fudan University for providing the gift of PANX1 antibody. We would like to thank Dr. Yongfeng Wang and Dr. Liquan Zhou from Institute of Reproductive Health, Huazhong University of Science and Technology for the help of mice microinjection. We also thank the patients and their family for their participation and support in this study. We also thank Experimental Medicine Center of Tongji Hospital, Tongji Medical School, Huazhong University of Science and Technology for animal feeding.

Author contributions
Juepu Zhou: Literature review, mouse experiment. Ruolin Mao: Literature review, human experiment. Meng Wang: Lead for prediction model, literature review, writing and revising. Rui Long: Tables, figures, literature review. Limin Gao: Literature review and revising. Xiangfei Wang: Literature review and revising. Lixia Zhu: Conception and design, writing and revising. Lei Jin: Primary supervisor, conception and design, writing and revising.

Funding
This work was supported by National Natural Science Foundation of China (82401948), Natural Science Foundation of Hubei Province (2024AFB052), Grant 2021YFC2700603 from the National Key Research & Development Program of China and Grant by the Key Research of Huazhong University of Science and Technology, Tongji Hospital (2022A20).

Data availability
No datasets were generated or analysed during the current study.

Declarations

Ethical approval
This study was approved by the ethics committee on human subject research at Tongji Hospital, Huazhong University of Science and Technology (TJ-IRB20220450). The animal experiments were approved by the Animal Welfare and Ethics Committee of Tongji Hospital (TJH-202210011).

Conflict of interest
All the authors declare no competing interests.

Received: 2 March 2024 / Accepted: 18 June 2024
Published online: 04 September 2024

References

1. Matzuk MM, Lamb DJ. The biology of infertility: research advances and clinical challenges. Nat Med. 2008;14(11):1197–213.
2. Shamseldin HE, Tulbah M, Kurdi W, Nemer M, Alsahan N, Al Mardawi E, et al. Identification of embryonic lethal genes in humans by autozygosity mapping and exome sequencing in consanguineous families. Genome Biol. 2015;16(1):116.
3. Webster A, Schuh M. Mechanisms of Aneuploidy in Human Eggs. Trends Cell Biol. 2017;27(1):55–68.
4. Yatsenko SA, Rajkovic A. Genetics of human female infertility†. Biol Reprod. 2019;101(3):549–66.
5. Inhorn MC, Patrizio P. Infertility around the globe: new thinking on gender, reproductive technologies and global movements in the 21st century. Hum Reprod Update. 2015;21(4):411–26.
6. Sang Q, Zhou Z, Mu J, Wang L. Genetic factors as potential molecular markers of human oocyte and embryo quality. J Assist Reprod Genet. 2021;38(5).
7. Christou-Kent M, Kherraf Z-E, Amiri-Yekta A, Le Blévec E, Karaouzène T, Conne B et al. PATL2 is a key actor of oocyte maturation whose invalidation causes infertility in women and mice. EMBO Mol Med. 2018;10(5).
8. Liu Z, Zhu L, Wang J, Luo G, Xi Q, Zhou X, et al. Novel homozygous mutations in PATL2 lead to female infertility with oocyte maturation arrest. J Assist Reprod Genet. 2020;37(4):841–7.
9. Feng R, Sang Q, Kuang Y, Sun X, Yan Z, Zhang S, et al. Mutations in TUBB8 and human oocyte meiotic arrest. N Engl J Med. 2016;374(3):223–32.
10. Liu Z, Xi Q, Zhu L, Yang X, Jin L, Wang J, et al. TUBB8 mutations cause female infertility with large Polar body oocyte and fertilization failure. Reprod Sci. 2021;28(10):2942–50.
11. Xu Y, Shi Y, Fu J, Yu M, Feng R, Sang Q, et al. Mutations in PADI6 cause female infertility characterized by early embryonic arrest. Am J Hum Genet. 2016;99(3):744–52.
12. Whyte-Fagundes P, Zoidl G. Mechanisms of pannexin1 channel gating and regulation. Biochim Biophys Acta Biomembr. 2018;1860(1):65–71.
13. Penuela S, Bhalla R, Gong X-Q, Cowan KN, Celetti SJ, Cowan BJ, et al. Pannexin 1 and pannexin 3 are glycoproteins that exhibit many distinct characteristics from the connexin family of gap junction proteins. J Cell Sci. 2007;120(Pt 21):3772–83.
14. Idzko M, Ferrari D, Eltzschig HK. Nucleotide signalling during inflammation. Nature. 2014;509(7500):310–7.
15. Furlow PW, Zhang S, Soong TD, Halberg N, Goodarzi H, Mangrum C, et al. Mechanosensitive pannexin-1 channels mediate microvascular metastatic cell survival. Nat Cell Biol. 2015;17(7):943–52.
16. Thompson RJ, Zhou N, MacVicar BA. Ischemia opens neuronal gap junction hemichannels. Science. 2006;312(5775):924–7.
17. Karatas H, Erdener SE, Gursoy-Ozdemir Y, Lule S, Eren-Koçak E, Sen ZD, et al. Spreading depression triggers headache by activating neuronal Panx1 channels. Science. 2013;339(6123):1092–5.
18. Sang Q, Zhang Z, Shi J, Sun X, Li B, Yan Z, et al. A pannexin 1 channelopathy causes human oocyte death. Sci Transl Med. 2019;11:485.
19. Wang W, Qu R, Dou Q, Wu F, Wang W, Chen B, et al. Homozygous variants in PANX1 cause human oocyte death and female infertility. Eur J Hum Genet. 2021;29(9):1396–404.
20. Wu X-W, Liu P-P, Zou Y, Xu D-F, Zhang Z-Q, Cao L-Y, et al. A novel heterozygous variant in PANX1 is associated with oocyte death and female infertility. J Assist Reprod Genet. 2022;39(8):1901–8.
21. Zhou J, Wang M, Hu J, Li Z, Zhu L, Jin L. A novel heterozygous variant in PANX1 causes primary infertility due to oocyte death. J Assist Reprod Genet. 2023;40(1):65–73.
22. Zhou X, Zhu L, Hou M, Wu Y, Li Z, Wang J, et al. Novel compound heterozygous mutations in WEE2 causes female infertility and fertilization failure. J Assist Reprod Genet. 2019;36(9):1957–62.
23. Elliott MR, Chekeni FB, Trampont PC, Lazarowski ER, Kadl A, Walk SF, et al. Nucleotides released by apoptotic cells act as a find-me signal to promote phagocytic clearance. Nature. 2009;461(7261):282–6.
24. Qu R, Dong L, Zhang J, Yu X, Wang L, Zhu S. Cryo-EM structure of human heptameric pannexin 1 channel. Cell Res. 2020;30(5):446–8.

25. Zhang S, Yuan B, Lam JH, Zhou J, Zhou X, Ramos-Mandujano G, et al. Structure of the full-length human Pannexin1 channel and insights into its role in pyroptosis. Cell Discovery. 2021;7(1):30.
26. Deng Z, He Z, Maksaev G, Bitter RM, Rau M, Fitzpatrick JAJ, et al. Cryo-EM structures of the ATP release channel pannexin 1. Nat Struct Mol Biol. 2020;27(4):373–81.
27. Rusiecka OM, Tournier M, Molica F, Kwak BR. Pannexin1 channels-a potential therapeutic target in inflammation. Front Cell Dev Biol. 2022;10:1020826.
28. Filiberto AC, Spinosa MD, Elder CT, Su G, Leroy V, Ladd Z, et al. Endothelial pannexin-1 channels modulate macrophage and smooth muscle cell activation in abdominal aortic aneurysm formation. Nat Commun. 2022;13(1):1521.
29. Huang G, Bao J, Shao X, Zhou W, Wu B, Ni Z, et al. Inhibiting pannexin-1 alleviates sepsis-induced acute kidney injury via decreasing NLRP3 inflammasome activation and cell apoptosis. Life Sci. 2020;254:117791.
30. Penuela S, Simek J, Thompson RJ. Regulation of pannexin channels by post-translational modifications. FEBS Lett. 2014;588(8):1411–5.
31. Zhao H-B, Zhu Y, Liang C, Chen J. Pannexin 1 deficiency can induce hearing loss. Biochem Biophys Res Commun. 2015;463(1–2):143–7.
32. Qian J, Nguyen NMP, Rezaei M, Huang B, Tao Y, Zhang X, et al. Biallelic PADI6 variants linking infertility, miscarriages, and hydatidiform moles. Eur J Hum Genet. 2018;26(7):1007–13.
33. Cao Q, Zhao C, Zhang X, Zhang H, Lu Q, Wang C et al. Heterozygous mutations in ZP1 and ZP3 cause formation disorder of ZP and female infertility in human. J Cell Mol Med. 2020;24(15):8557-66.

Publisher's Note